Calibration of WindSat Polarimetric Channels With a Vicarious Cold Reference

Christopher S. Ruf, *Fellow, IEEE*, Ying Hu, and Shannon T. Brown

***Abstract*—Absolute calibration of WindSat's third and fourth Stokes brightness temperatures (T_3 and T_4) is needed at the tenth of Kelvin level in order to adequately resolve their dependence on wind direction. Previous aircraft based fully polarimetric microwave radiometers have generally relied on "circle flights," during which a single area of the ocean is observed at all azimuth angles, to estimate residual biases in the calibration of its polarimetric channels. WindSat, the first spaceborne fully polarimetric microwave radiometer, operates in low earth orbit and thus cannot execute this traditional calibration technique. A new method is presented to estimate the residual biases that are present in WindSat's T_3 and T_4 estimates. The method uses a vicarious cold reference brightness temperature applied to measurements made by WindSat at $\pm 45^\circ$ slant linear (T_P and T_M) and left- and right-hand circular (T_L and T_R) polarization. WindSat derives the third and fourth Stokes brightness temperatures by the differences $T_P - T_M$ and $T_L - T_R$, respectively. The method is demonstrated by applying it to the 10.7-GHz WindSat observations. Calibration biases of 0.2–0.6 K are determined with a precision of 0.04 K.**

***Index Terms*—Calibration, microwave radiometry.**

I. Introduction

THE National Polar-orbiting Operational Environmental Satellite System (NPOESS) is a new initiative jointly sponsored by the U.S. Government's NASA, NOAA, and Department of Defense agencies. It is intended to promote the development and operation of a next generation of Earth environmental monitoring satellites that can be shared by scientific, operational, and defense users. Coriolis, a proof-of-concept and risk mitigation mission, was successfully launched on January 6, 2003 carrying the WindSat instrument. WindSat is a first-of-its-kind spaceborne microwave radiometer that can remotely sense the speed and direction of near surface winds over the ocean by making fully polarimetric observations of the complete Stokes brightness temperature vector. A detailed description of the instrument is given by Gaiser *et al.* [5].

WindSat measures the full polarimetric Stokes brightness temperature (T_B) vector at 10.7, 18.7, and 37.0 GHz and vertical and horizontal polarizations only at 6.8 and 23.8 GHz. For the fully polarimetric channels, one antenna feed orthomode transducer (OMT) is used to form vertical and horizontal linear polarizations, a second OMT forms $+45^\circ$ and -45° slant linear polarizations, and a third OMT forms left-hand and right-hand circular polarizations. This OMT method directly measures the T_B at six individual polarization states using conventional incoherent square law detectors. These measurements, once calibrated as T_Bs, are referred to as T_V, T_H, T_P, T_M, T_L, and T_R, respectively. Third and fourth Stokes T_Bs are then generated by

$$T_3 = T_P - T_M$$
$$T_4 = T_L - T_R. \tag{1}$$

Generation of the third and fourth Stokes T_Bs in this manner has several advantages. It permits the use of standard, square law detector based, radiometer receivers that are well understood in terms of component and subsystem design and system calibration. The six individual polarization T_Bs are calibrated before and after Earth observations by measurements pointed at an ambient black body load and a cold (~ 2.7 K) space reflector. This calibration method is adopted directly from the SSM/I approach [6].

The OMT method is also a good way to reduce biases in the calibration of T_3 and T_4 [11]. Calibration biases that are common to T_P and T_M or to T_L and T_R will cancel out in (1). The single largest contributor to T_B biases for many radiometers is inaccurate accounting for antenna sidelobe contributions. Mechanical and electrical symmetries in the WindSat antenna design between both pairs of channels that are differenced in (1) will give rise to a common mode bias that is removed by the differencing operation. The residual biases that remain in T_3 and T_4 should generally be smaller than those in the original six polarization channels. However, even errors as small as a few tenths of Kelvins can be problematic for wind direction retrieval algorithms.

The sensitivity of the retrieval of wind direction to calibration biases in T_3 and T_4 can be estimated by considering the geophysical model functions (GMFs) that relate them. A number of GMFs have been developed from both theoretical and experimental considerations and they generally exhibit similar behavior [8], [12], and [15]. For illustrative purposes, we consider one such model, derived from a large ensemble of QuikScat wind vector measurements coincident in time and space with WindSat T_B measurements [1]. At 10.7 GHz and with a wind speed of 7 m/s, the third Stokes T_B can be modeled as

$$T_3 = -0.3 \sin\phi - 0.5 \sin 2\phi \tag{2}$$

where ϕ is the relative azimuth angle between the look direction of the radiometer and the wind direction. The greatest rate

Manuscript received February 10, 2005; revised May 11, 2005. This work was funded in part by the Naval Research Laboratory under Award N00173-03-1-G008.

C. S. Ruf is with the Space Physics Research Laboratory, Department of Atmospheric, Oceanic, and Space Sciences, University of Michigan, Ann Arbor, 48109 MI USA (e-mail: cruf@umich.edu).

Y. Hu was with the Space Physics Research Laboratory, Department of Atmospheric, Oceanic, and Space Sciences, University of Michigan, Ann Arbor, 48109 MI USA. She is currently with the Institute for Social Research, University of Michigan, Ann Arbor, MI 48109 USA (e-mail: ihu@isr.umich.edu).

S. T. Brown is with the Micrwoave Advanced Systems, Jet Propulsion Laboratory, Pasadena, CA 91109 USA (e-mail: shannon.t.brown@jpl.nasa.gov).

Digital Object Identifier 10.1109/TGRS.2005.855996

of change of T_3 with wind direction occurs at $\phi = 0°$, at which point $(dT_3/d\phi)^{-1} = -44.1°/\text{K}$. Under these conditions, a 10° change in wind direction would correspond to a 0.23-K change in T_3. This is one simple illustration of the fact that fairly small errors in T_3, at the few tenths of Kelvins level, can be associated with errors in retrieved wind direction on the order of 10°. In practice, with actual wind vector retrieval algorithms, the sensitivity to calibration errors can be even greater than this because of other complications of the retrieval such as atmospheric corrections and multivalued solutions for wind direction.

A method is presented here that estimates the calibration bias present in third and fourth Stokes T_Bs from an ensemble of Earth observations. It is demonstrated using WindSat measurements at 10.7 GHz for illustrative purposes but can (and has) been successfully applied to all of WindSat's polarimetric channels. The method adopts a vicarious calibration technique that was developed previously for estimating biases in conventional linearly polarized measurements of T_B. A brief review of the vicarious cold reference approach is given in Section II. Section III describes details of its application to the WindSat case. Section IV presents results—estimating the sign and magnitude of the calibration biases and the error in that estimate.

II. Vicarious Cold Reference

The vicarious cold reference temperature represents a statistical lower bound on T_B for an Earth viewing radiometer. It works at microwave frequencies below the 60-GHz oxygen absorption lines and is especially applicable in the microwave atmospheric window channels at which the WindSat fully polarimetric channels operate. Minimum T_Bs occur under clear skies and calm sea surface conditions at a particular sea surface temperature (SST). The optimum SST, as well as the value of the lower bound on T_B, depends on frequency and Earth incidence angle. The exact combination of conditions needed to produce the minimum T_B does not ever need to be present in order for this calibration method to work. It is sufficient merely that the lower bound exist in principle and that the probability distribution of a large ensemble of the colder T_B observations tend to cluster near it. The technique has been used previously to characterize calibration biases present in conventional linear polarization spaceborne radiometers [2], [10].

The vicarious cold reference T_B is determined from a large ensemble of T_B observations by statistical means. First, a histogram of the T_Bs is formed, with particular attention paid to measurements within 10 K of the theoretical lower bound. An inverse cumulative distribution function, $f(p)$, is derived from the histogram which has the property that p percent of the T_Bs in the ensemble are less than or equal to a brightness temperature of $f(p)$. A third order polynomial in p is best fit by least squares regression to the region of $f(p)$ near the lower bound of T_B (the region $3\% < p < 10\%$ is used in the analysis presented here). The polynomial has the form

$$f(p) \approx a_0 + a_1 p + a_2 p^2 + a_3 p^3. \tag{3}$$

The zeroth coefficient, a_0 in (3), represents the polynomial approximation of the value of T_B below which there are 0% of the ensemble of observations (i.e., $a_0 = f(p = 0\%)$. The zeroth coefficient is the vicarious cold reference. The calibration bias of a linearly polarized radiometer channel is determined as the difference between the vicarious cold reference and the theoretical lower bound on T_B at that channel's frequency and incidence angle. Details of the development of this algorithm and of its characterization are given in [10].

The vicarious cold reference, when used with linearly polarized radiometer channels in the microwave atmospheric windows, has been shown to be repeatable over many years to better than 0.4 K [9]. This allows the long-term stability of an instrument to be closely tracked. While this ensures that relative calibration biases can be removed between measurements at different times, determining the absolute calibration bias at a particular time is more problematic. The value of the theoretical lower bound on T_B is largely determined by the dielectric constant of the sea water for the sea surface temperature at which the T_B is a minimum. There are a number of dielectric models in the literature [4], [7], [13], [14] and the T_Bs they predict generally disagree at the ~ 1 Kelvin level at the WindSat frequencies. This level of uncertainty limits our ability to determine the true lower bound on T_B and, hence, the true calibration bias of a linearly polarized radiometer channel. The situation is markedly different for the case of third and fourth Stokes T_Bs that are generated by the OMT method. The theoretical lower bound on T_B at each of the directly measured polarizations—T_P, T_M, T_L, and T_R—should equal the arithmetic average of the vertically and horizontally polarized lower bound T_Bs. The difference between any two of these lower bounds should be zero regardless of which dielectric model is correct. When actual WindSat data are processed, a nonzero difference between the vicarious cold references at T_P and T_M, for example, would indicate a calibration bias in T_3.

III. WindSat Processing for Vicarious Cold Reference

The vicarious cold reference is dependent on the incidence angle of an observation. WindSat is a conically scanning instrument with an axis of rotation that is nominally oriented along the local nadir direction. Perfect alignment would produce a constant incidence angle at the Earth surface for all azimuthal scan positions. In practice, small geometrical misalignments result in a variation of the incidence angle with scan position. The effect of the variations on calibration by vicarious cold reference must be accounted for. An example of the behavior of the varying incidence angle is shown in Fig. 1. Incidence angles are higher in the fore portion of the scan and lower in the aft portion, suggesting that the rotation axis has a predominant misalignment in pitch. Overall variations in incidence angle for the 10.7-GHz channel range between 49.5° and 50.6°.

The effect of variations in incidence angle on the vicarious cold reference is assessed via a Monte Carlo simulation. An ensemble of simulated WindSat T_Bs was generated using a clear sky forward radiative transfer model. Ocean emissivity was modeled using the Stogryn [14] dielectric model. A database of atmospheric radiosonde profiles, covering 56 globally distributed island launch sites, was used to derive atmospheric upwelling and downwelling emission and transmissivity. Near-surface air temperatures from the atmospheric profiles were used as a surrogate for SST. Ocean salinity was selected from an objectively analyzed global one-by-one degree

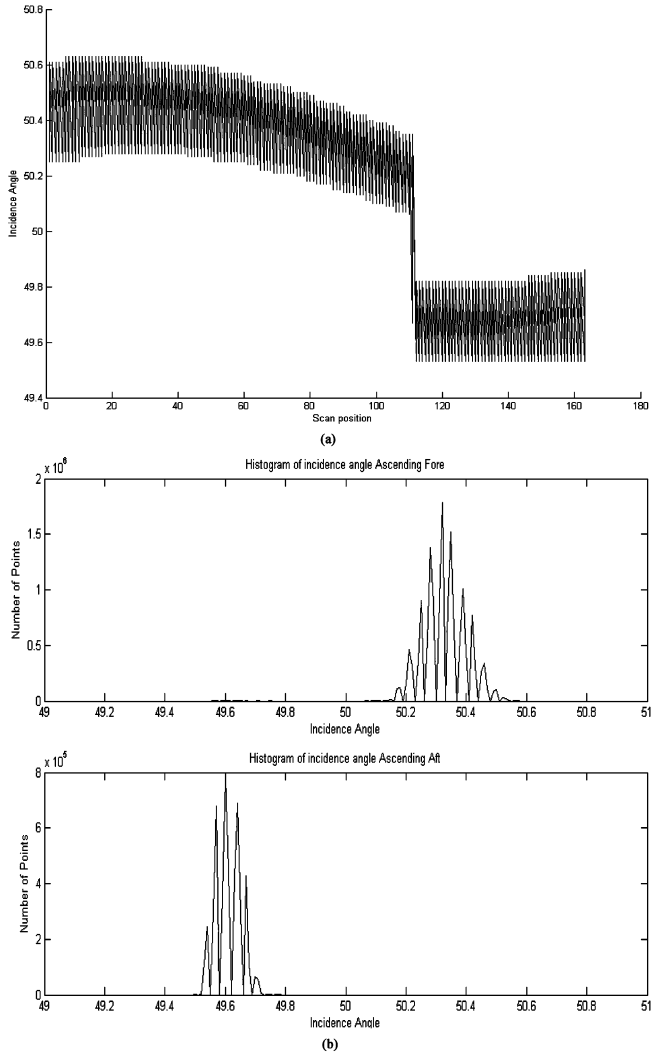

Fig. 1. (a) Typical example of the variation in Earth incidence angle of WindSat observations at 10.7 GHz over ~ 200 azimuthal revolutions. The x axis (scan position) is an index of azimuthal rotation angle. Scan positions below 112 represent the fore portion of the scan. Positions greater than 115 represent the aft portion of the scan. (b) Histogram of incidence angles in (top) the fore and (bottom) aft portions of the scan.

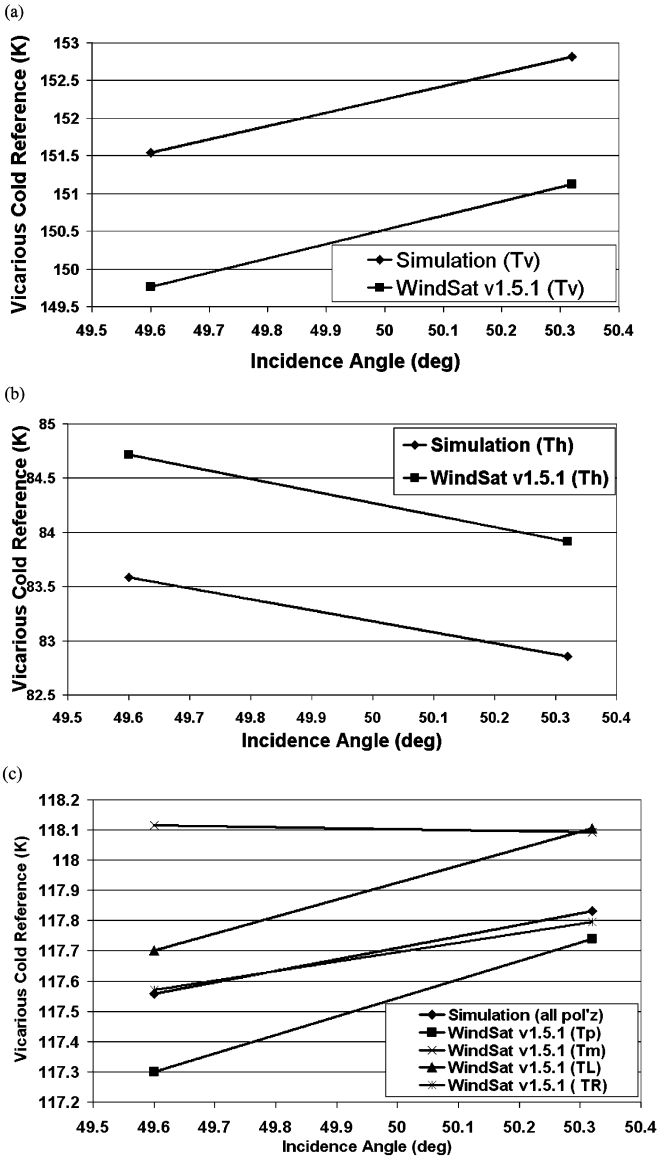

Fig. 2. Simulated and actual WindSat-derived vicarious cold reference (VCR) brightness temperatures at 10.7 GHz generated separately from T_B observations in the for and aft portions of the scan for (a) vertical, (b) horizontal, and (c) $\pm 45^\circ$ slant linear and left/right-hand circular polarizations. Incidence angles shown are the average values over each portion of the scan.

grid during 1998 that was assembled by the NOAA National Oceanographic Data Center [3]. Ocean surface wind speed was selected randomly from a Rayleigh distribution with a mean value of 7 m/s. Most importantly, the incidence angle of observations was selected randomly from the empirical probability distribution (shown in Fig. 1) of actual WindSat values. The resulting simulated T_Bs were separated into two groups, corresponding to the fore and aft distributions of incidence angle, and applied to the vicarious cold reference algorithm. The results are shown in Fig. 2 at 10.7 GHz.

In Fig. 2, two sets of vicarious cold reference T_Bs are shown for each polarization. One set is derived from the Monte Carlo simulation described above. The other is derived from WindSat measurements (calibrated using the Naval Research Laboratory version 1.5.1 ground processing algorithm), which were also separated into fore and aft scan subsets. In the figure, each line is defined by its two end points. The T_B values of the end points are determined by applying the vicarious cold reference algorithm to ensembles of T_Bs (either simulated or measured) which have the fore and aft statistical distributions of incidence angles shown in Fig. 1. The incidence angle values of the end points are the expected values of those distributions. The absolute error in the individual T_B values of the end points may be as large as ~ 1 K for the simulated data due to uncertainties in the ocean dielectric model. However, for purposes of this analysis, a more relevant consideration is the relative error of T_B values between polarization channels. Model dependent errors will be common between T_P, T_M, T_L, and T_R channels so the relative error should be much lower than 1 K. An assessment of the accuracy of this calibration method is presented in Section IV.

Fig. 2(a) shows the results for vertical polarization at 10.7 GHz. The dependence on incidence angle of both the simulated and WindSat vicarious cold references are similar, with a slope of approximately 1.8 Kelvin/degree. There is a consistent bias of approximately 1.7 K (WindSat lower)

between the simulated and measured T_Bs at all incidence angles. For horizontal polarization [Fig. 2(b)], the dependence on incidence angle is approximately -1.1 Kelvin/degree for both simulated and WindSat T_Bs. A bias is also evident here, with WindSat consistently ~ 1.1 K lower than the simulations. Offsets in vertical (V-pol) and horizontal polarization (H-pol) T_Bs between the simulations and observations are likely due to some combination of small WindSat calibration biases together with small errors in the simulation model.

The vicarious cold references at the other four polarizations are shown in Fig. 2(c). A single simulation result is shown that is common to all four polarizations, since the vicarious cold reference should in theory be the same for T_P, T_M, T_L, and T_R. The 0.5-Kelvin/degree dependence on incidence angle is intermediate between that of V- and H-pol since the vicarious cold reference is their arithmetic mean. WindSat results at T_P, T_L, and T_R show a small positive dependence on incidence angle and T_M is nearly independent of incidence angle. Most noteworthy is the fact that there are offsets in Fig. 2(c) between the average WindSat results at each polarization. These offsets hold the key to estimating calibration biases in T_3 and T_4.

IV. Results

The bias in calibration of WindSat's T_3 estimates is estimated as the difference between the vicarious cold references derived from its measurements of T_P and T_M. Similarly, T_4 biases are the difference between T_L and T_R vicarious cold references. An average calibration bias over all incidence angles is estimated by averaging the difference in vicarious cold reference at high and low incidence angles. In this way, the T_3 and T_4 biases are determined to be -0.63 and 0.21 K, respectively.

In order to assess the accuracy of the vicarious cold reference determination of T_3 and T_4 biases, a second calibration method is needed. The conventional method for determining T_3 and T_4 biases with airborne polarimetric radiometers is to perform "circle flights" [12], [15]. An airplane is flown in a circle at a constant bank angle while the radiometer's antenna beam is pointed at the ocean near the center of the circle. The resulting time series of T_3 is a continuously varying function of ϕ in (2) and so traces out the double harmonic sinusoidal behavior of the function. The presence of a calibration bias is immediately evident as a constant offset in the sinusoidal dependence. A calibration that is roughly analogous to the airborne circle flight can be constructed for WindSat by assembling a large database of WindSat T_B observations that are colocated in time and space with surface measurements of wind speed and direction. This has been done using NOAA National Data Buoy Center (NDBC) buoys as surface truth. The buoy data were matched up against WindSat overpasses within 25 km and 10 min of coincidence. Match ups were further filtered, using the WindSat derived atmospheric retrievals described in [1], to have precipitable cloud liquid water content of less than 1.0 mm and integrated water vapor burden of less than 7 cm. This essentially screens out any extremely cloudy or precipitating conditions. The colocated database is large enough that a wide range of relative wind speeds and directions are included. Scatter plots of T_3 or T_4 versus wind direction within a narrow range of wind

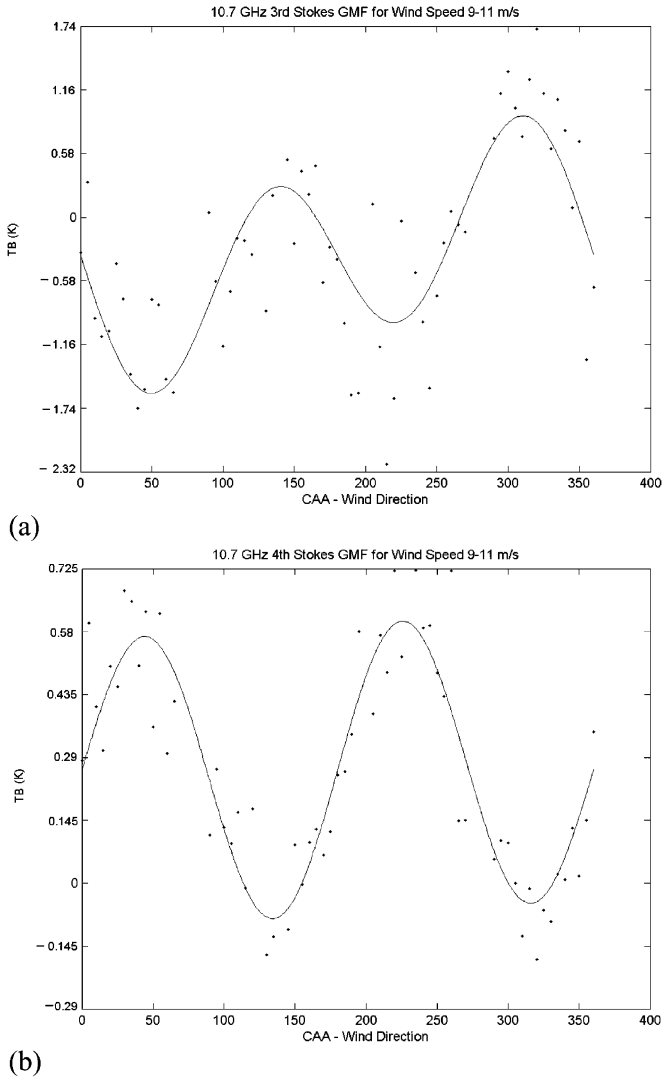

Fig. 3. Scatter plot of global WindSat (a) T_3 and (b) T_4 matchups with NDBC buoy measurements of wind direction for wind speeds between 9 and 11 m/s. The solid line represents a least squares fit by a double harmonic sinusoid. The scatter plot exhibits a nonzero mean value due to calibration biases. Buoy (or other ground truth) matchups of this type are the spaceborne analog to the airborne "circle flight" for determining calibration biases in the hardware.

speeds should largely reproduce the calibrating feature of the airborne circle flights. Unlike the airborne case, however, there will also be variations in the atmospheric conditions between data points. Because the conditions should be largely uncorrelated with wind direction, atmospheric variations will increase the scatter in the plots but should not introduce any offset that could be misinterpreted as a calibration bias. An example of such scatter plots is shown in Fig. 3 at 10.7 GHz for moderate (9–11 m/s) wind speeds. The signal exhibits the expected double harmonic sinusoidal variation as a function of relative wind direction. There are also clear shifts in the average value of the signals away from zero. These are caused by biases in the calibration of T_3 and T_4. The biases determined in this way can be compared to those found using the vicarious cold reference method. The biases in T_3 and T_4 found from the NDBC matchups are -0.66 and 0.22 K, respectively. These results compare vary favorably with those found earlier.

TABLE I
CALIBRATION BIASES PRESENT IN WINDSAT'S THIRD AND FOURTH STOKES BRIGHTNESS TEMPERATURES AS DETERMINED BY TWO DIFFERENT METHODS: 1) VICARIOUS COLD REFERENCE DIFFERENCES BETWEEN $\pm 45^\circ$ SLANT LINEARLY POLARIZED AND LEFT- AND RIGHT-HAND CIRCULARLY POLARIZED BRIGHTNESS TEMPERATURES AND 2) CONSTANT TERM IN SINUSOIDAL FIT TO RELATIVE WIND DIRECTION OF A LARGE DATABASE OF WINDSAT MEASUREMENTS COLOCATED WITH NDBC BUOY SURFACE TRUTH

Calibration Biases in WindSat Brightness Temperatures

	Vicarious Cold Reference	NDBC Buoy Matchups
version 1.5.1 processing		
T_3	-0.63 K	-0.66 K
T_4	0.21 K	0.22 K
version 1.6.1 processing		
T_3	-0.29 K	-0.27 K
T_4	0.19 K	0.27 K

The results presented thus far are all based on WindSat T_B measurements that have been calibrated using the Naval Research Laboratory's version 1.5.1 ground processing. Version 1.6.1 ground processing produces slightly different T_Bs. The most significant difference between the two versions, in terms of the absolute calibration of the T_Bs, was changes to the integrated sidelobe beam fractions that are assumed in the sidelobe correction algorithm. A second comparison between the vicarious cold reference and the NDBC buoy matchup approaches to estimating the calibration bias was performed using version 1.6.1 ground processing. Those results, together with the results with version 1.5.1 processing, are listed in Table I. In both cases, bias determinations are very consistent between the two methods. This suggests that the vicarious cold reference method is capable of tracking changes in calibration bias. The RMS difference between the two methods, averaged over T_3 and T_4 and over both versions of ground processing, is 0.04 K.

V. CONCLUSION AND DISCUSSION

The difference between WindSat's vicarious cold reference brightness temperature measurements at $\pm 45^\circ$ slant linear polarization is one way to determine the bias present in calibration of the third Stokes brightness temperature. Similarly, differences at left- and right-hand circular polarization determine the bias in the fourth Stokes brightness temperature. The bias determinations are consistent at the 0.04-K level with another method that uses surface truth buoy matchups to approximate the circle flight method of calibration that is commonly employed with airborne fully polarimetric radiometers. The vicarious cold reference method has several advantages. It requires measurements taken over a relatively short period of time to adequately estimate the necessary lower bound statistics. The results presented in [10], for example, use data acquired over ten-day periods to produce estimates of the vicarious cold reference with ~ 0.3 K RMS error. Shorter time periods have greater uncertainty because the vicarious cold reference is a statistic derived from a finite population of T_B samples. Use of data acquired over much longer time periods runs the risk of averaging over slowly time varying calibration biases. For the results presented above, WindSat measurements were used from the time period August 31, 2003 through September 28, 2003. Buoy matchups, on the other hand, generally require a longer time period to provide enough colocated measurements—with a sufficient distribution of relative wind directions inside a narrow enough interval of wind speeds—to adequately estimate the constant term in a least squares sinusoidal fit. The WindSat/buoy data used here were assembled over the time period September 1, 2003 through December 17, 2003. The shorter time required means that changes in calibration are better able to be tracked. The data processing that is needed for vicarious calibration is also considerably simpler since it involves only a single data set. Furthermore, the vicarious cold reference method, since it is applied to the T_P/T_M and T_L/T_R channels individually and then differenced, may provide clues as to which channel is in need of calibration. Individual channel comparisons with the vicarious cold reference could confidently identify only large calibration errors since the error in the reference due to dielectric model uncertainties is approximately 1 K. The dependence of the vicarious cold reference on incident angle is another tool for assessing the calibration of individual channels. For example, the behavior of T_M versus incidence angle in Fig. 2(c) suggests that it has a scan-angle-dependent calibration bias. By comparison, the buoy method does not provide information on the individual channels that are differenced in (1).

The wind direction retrieval requirements on absolute calibration of the third and fourth Stokes brightness temperatures can be quite severe, particularly for lower wind speeds at which changes in T_B with wind direction are very small. Biases in T_3 or T_4 of as little as a few tenths of a Kelvin can be significant. The vicarious cold reference method has shown the ability to identify and track these calibration biases at levels as low as 0.04 K. And, once identified, it is a relatively simple matter to remove biases from the measurements in the ground processing.

REFERENCES

[1] S. T. Brown, C. S. Ruf, and D. R. Lyzenga, "An emissivity-based wind vector retrieval algorithm for the WindSat polarimetric radiometer," *IEEE Trans. Geosci. Remote Sens.*, vol. 44, no. 3, pp. 611–621, Mar. 2006.
[2] S. Brown, C. Ruf, S. Keihm, and A. Kitiyakara, "Jason microwave radiometer performance and on-orbit calibration," *Marine Geodesy*, vol. 27, no. 1–2, pp. 199–220, 2004.
[3] M. Conkright, S. Levitus, T. O'Brien, T. Boyer, J. Antonov, and C. Stephens. (1998) World Ocean Atlas 1998 CD-ROM Data Set Documentation.
[4] W. Ellison, A. Balana, G. Delbos, K. Lamkaouchi, L. Eymard, C. Buillou, and C. Prigent, "New permittivity measurements of seawater," *Radio Sci.*, vol. 33, no. 3, pp. 639–648, 1998.
[5] P. Gaiser, K. M. St. Germain, E. M. Twarog, G. A. Poe, W. Purdy, D. Richardson, W. Grossman, W. L. Jones, D. Spencer, G. Golba, J. Cleveland, L. Choy, R. M. Bevilacqua, and P. S. Chang, "The WindSat spaceborne polarimetric microwave radiometer: Sensor description and early orbit performance," *IEEE Trans. Geosci. Remote Sens.*, vol. 42, no. 11, pp. 2347–2361, Nov. 2004.
[6] J. P. Hollinger, J. L. Pierce, and G. A. Poe, "SSM/I instrument evaluation," *IEEE Trans. Geosci. Remote Sens.*, vol. 28, no. 5, pp. 781–790, Sep. 1990.
[7] L. A. Klein and C. T. Swift, "An improved model for the dielectric constant of sea water at microwave frequencies," *IEEE Trans. Antennas Propagat.*, vol. AP-25, pp. 104–111, 1976.
[8] J. Piepmeier and A. Gasiewski, "High-resolution passive polarimetric microwave mapping of the ocean surface wind vector fields," *IEEE Trans. Geosci. Remote Sens.*, vol. 39, no. 3, pp. 606–622, Mar. 2001.

[9] C. S. Ruf, "Characterization and correction of a drift in calibration of the TOPEX microwave radiometer," *IEEE Trans. Geosci. Remote Sens.*, vol. 40, no. 2, pp. 509–511, Feb. 2002.
[10] ——, "Detection of calibration drifts in spaceborne microwave radiometers using a vicarious cold reference," *IEEE Trans. Geosci. Remote Sens.*, vol. 38, no. 1, pp. 44–52, Jan. 2000.
[11] ——, "Constraints on the polarization purity of a Stokes microwave radiometer," *Radio Sci.*, vol. 33, no. 6, pp. 1617–1639, 1998.
[12] N. Skou and B. Laursen, "Measurement of ocean wind vector by an airborne, imaging polarimetric radiometer," *Radio Sci.*, vol. 33, no. 3, pp. 669–675, 1998.
[13] A. Stogryn, "Equations for calculating the dielectric constant of saline water," *IEEE Trans. Microw. Theory Tech.*, vol. MTT-19, pp. 733–736, 1971.
[14] ——, "Equations for the permittivity of sea water," Nav. Res. Lab., Washington, DC, 1997.
[15] S. H. Yueh, W. J. Wilson, S. V. Nghiem, F. K. Li, and W. B. Ricketts, "Polarimetric measurements of sea surface brightness temperature using an aircraft K-band radiometer," *IEEE Trans Geosci. Remote Sens.*, vol. 33, no. 1, pp. 85–92, Jan. 1995.

Christopher S. Ruf (S'85–M'87–SM'92–F'01) received the B.A. degree in physics from Reed College, Portland, OR, and the Ph.D. degree in electrical and computer engineering from the University of Massachusetts, Amherst.

He is currently a Professor of atmospheric, oceanic, and space sciences and electrical engineering and computer science at the University of Michigan, Ann Arbor. He has worked previously as a Production Engineer for Intel Corporation, Santa Clara, CA, as a member of the technical staff for the Jet Propulsion Laboratory, Pasadena, CA, and as a member of the faculty at Pennsylvania State University, University Park. During 2000, he was a Guest Professor at the Technical University of Denmark, Lyngby. His research interests involve microwave remote sensing instrumentation and geophysical retrieval algorithms. He is currently involved with spaceborne radiometers on the current TOPEX, GeoSat Follow-on, Jason, and WindSat and the upcoming CMIS, Aquarius, and Juno missions. He has published over 87 refereed articles and is a past Associate Editor and Guest Editor for *Radio Science*.

Dr. Ruf has received three NASA Certificates of Recognition and four NASA Group Achievement Awards, as well as the 1997 GRS-S Transactions Prize Paper Award and the 1999 IEEE Judith A. Resnik Technical Field Award. He is a past Editor of the IEEE GRS-S Newsletter and currently an Associate Editor and Guest Editor of the IEEE TRANSACTIONS ON GEOSCIENCE AND REMOTE SENSING. He is a member of the AGU, AMS, and URSI Commission F.

Ying Hu received the B.S. degree in photogrammetry and remote sensing from Wuhan University, Wuhan, China, and the M.S. degree in atmospheric science from the University of Michigan, Ann Arbor, in 2002 and 2005, respectively.

She has worked for the Remote Sensing Laboratory, Wuhan University in the field of ground objects classification and edge detection of spaceborne and airborne hyperspectral images. From 2003 to 2005, she was a Graduate Student Research Assistant in the Spaceborne Microwave Remote Sensors Group, University of Michigan, involved in the WindSat and TOPEX/Poseidon projects with a focus on sensor calibration/validation and wind vector retrieval. She is currently with the Institute for Social Research, University of Michigan.

Shannon T. Brown received the B.S. degree in meteorology from Pennsylvania State University, University Park, and the M.S. degree in atmospheric science and the Ph.D. degree in geoscience and remote sensing from the University of Michigan, Ann Arbor, in 2001, 2003, and 2005, respectively.

He is a member of the engineering staff in the Microwave Advanced Systems Section, NASA Jet Propulsion Laboratory, Pasadena, CA. His research interests involve on-orbit calibration/validation and performance assessment of the Jason Microwave Radiometer and of the WindSat polarimetric microwave radiometer, development of an on-Earth hot calibration brightness temperature reference for satellite microwave radiometers, surface wind speed and rain rate retrieval algorithm development using airborne active and passive microwave measurements in rain, and development of a wind vector retrieval algorithm from space using the WindSat polarimetric microwave radiometer.

Dr. Brown is the recipient of a 2004 NASA Group Achievement Award for his contribution to the UMich/GSFC Lightweight Rainfall Radiometer.